

Supporting Information

Sunlight Driven E-Z Isomerization of Liquid Crystals based on Hexahydroxytriphenylene Nano-templates for Enhanced Solid-state Solar Thermal Energy Storage

*Monika Gupta, * Ashy, and Abhinand Krishna KM*

Department of Chemistry, Indian Institute of Technology Ropar (IIT-Ropar), Bara Phool, Punjab-140001, India.

*Corresponding author: Tel.: +91-1881-232074; E-mail: monika.gupta@iitrpr.ac.in

Table of Contents

| S. No. | Contents | Page No. |
|--------|-----------------------|----------|
| 1 | Experimental Section | 2 - 5 |
| 2 | NMR spectra | 5 - 8 |
| 3 | TGA Analysis | 8 |
| 4 | DSC Analysis | 9 |
| 5 | POM &WAXS Studies | 9 - 10 |
| 6 | Photophysical Studies | 11 - 15 |
| 7 | Miscellaneous | 15 - 23 |
| 8 | References | 23 - 24 |

1. Experimental Section

1.1. Materials and Reagents

Chemicals and solvents were all of AR quality and were used without further purification. Chemicals were purchased from Sigma-Aldrich (Bangalore, India), TCI, and Avra Synthesis Pvt. Ltd. Column chromatographic separations were performed on silica gel (60-120, 100-200 & 230-400 mesh). Thin layer chromatography (TLC) was performed on aluminium sheets pre-coated with silica gel (Merck, Kieselgel 60, F254).

1.2. Synthesis and Characterization of Target Compounds

Compounds **5** and **7** were prepared according to the previous reports.^{1,2}

For the synthesis of final compounds **1-3**, respective compound **7** (0.83 g, 9 equivalents) was added in a dry single neck round bottom flask of 50 mL under argon and dissolved in butanone (25 ml). This was followed by adding K_2CO_3 (0.76 g, 18 equivalents) and stirring the mixture for 15 minutes. Compound **5** (0.5 g, 1 equivalent) and a catalytic amount of KI were added to the stirred mixture. The progress of the reaction was monitored by TLC. After the completion of the reaction (18 hours), the mixture was filtered to remove K_2CO_3 and evaporated under reduced pressure. The crude mixture was then purified by column chromatography using silica gel of mesh size 230-400. The pure products were eluted at 30 - 45% DCM in Hexane to obtain the final compounds.

All the synthesized compounds were characterized by 1H NMR, ^{13}C NMR, UV-vis, elemental analysis and mass spectrometry as shown below:

1.3. Instrumental

1.3.1. Structural characterization. Structural characterization of the compound was carried out through a combination of 1H NMR and ^{13}C NMR (Jeol JNM ECS 400 MHz NMR spectrometer), UV-vis spectroscopy (Shimadzu UV-2600 spectrophotometer), mass spectrometry (Bruker Daltonics *autoflex II*) and elemental analysis (EURO EA CHNS). NMR spectra were recorded using deuterated chloroform ($CDCl_3$) as solvent and tetramethylsilane (TMS) as an internal standard.

1.3.2. Thermogravimetric Analysis. Thermogravimetric analysis was carried out from 25 to 500 °C (at a heating rate of 10 °C min⁻¹) under nitrogen atmosphere on a TGA/DSC 1 instrument

with a SDTA sensor (Mettler-Toledo). The thermal data were analyzed in the STARe software (version 12.1).

1.3.3. Differential Scanning Calorimetry. DSC measurements were performed on a PerkinElmer DSC 8000 equipped with cryofill cooling system and Pt/Ir ovens. The samples were sealed in TA hermetic pans and lids. All measurements were performed with a rate of either 5 or 10 K/min and were evaluated with the Pyris Software for Windows.

1.3.4. Polarized Optical Microscopy. Textural observations of the mesophase were performed with Carl Zeiss Axio Imager A2m equipped with Hg arc lamp and filter cube, and LTS420 + LNP95 heating stage.

1.3.5. X-ray Diffraction. The temperature dependent WAXS investigations were performed on a Bruker Nanostar (Detector Vantec 2000, Microfocus copper anode X-ray tube Incoatec). Aligned samples were prepared by fiber extrusion method with a customized extruder. The aligned fibers were transferred to Mark capillaries, which were sealed and glued into the metal sample holder. The XRS heating system was calibrated by liquid crystal standard compounds. The XRS data was evaluated by the program datasqueeze using silver behenate as a calibration standard.

1.3.6. LED Irradiation. Photo irradiation studies was carried out using Holmarc HO-HBL-XY LED Irradiation setup with 365 nm, 395nm, 430 nm, 530 nm, 590 nm and 625 nm LED lights having a power of 36 mW/cm².

1.3.7. IR Thermal Imaging. IR Thermal Images of heat release from thin film samples were captured using FLIR One Edge Pro thermal camera in MSX mode.

1.3.8. Solar Power measurements. The intensity of sunlight inside the greenhouse was measured using Metravi 207 Solar Power Meter.

Compound 5

¹H NMR (400 MHz, CDCl₃, δ in ppm): 7.84 (s, 6H), 4.23 (t, 12H, J = 8 Hz), 3.40 (t, 12H, J = 8, 4 Hz), 1.94 (quint, 12H, J = 8, 4, 8, 8 Hz), 1.85 (quint, 12H, J = 4, 8, 8, 8 Hz), 1.61 - 1.25 (m, 72H).

Compound 7a

¹H NMR (400 MHz, CDCl₃, δ in ppm): 7.35 - 7.27 (m, 1H), 7.05 (t, 2H, J = 8 Hz), 6.53 (d, 2H, J = 10.4 Hz).

Compound 7b

¹H NMR (400 MHz, CDCl₃, δ in ppm): 7.43 (d, 1H, J = 8 Hz), 7.22 (t, 1H, J = 8 Hz), 6.96 (s, 2H), 6.74 (d, 1H, J = 2 Hz).

Compound 7c

¹H NMR (400 MHz, CDCl₃, δ in ppm): 7.40 (d, 2H, J = 8 Hz), 7.18 (t, 1H, J = 8 Hz), 6.57 (d, 2H, J = 8 Hz).

Compound 1 (0.38 g, Yield: 45%)

UV-vis (nm): 280, 322, 430.

¹H NMR (400 MHz, CDCl₃, δ in ppm): 7.82 (s, 6H), 7.17 (t, 4.54H, J = 4, 8 Hz), 7.02 (t, 1.45H, J = 8 Hz), 6.85 (t, 9H, J = 8 Hz), 6.57 (t, 2.99H, J = 8, 12 Hz), 6.45 (t, 1.97H, J = 8, 4 Hz), 6.36 (t, 10.09H, J = 12 Hz), 4.21 (s, 12.02H), 3.97 (t, 2.08H, J = 4, 8 Hz), 3.88 - 3.80 (m, 10.06H), 1.95 - 1.88 (m, 12.15H), 1.75 - 1.66 (m, 12.06H), 1.42 - 1.25 (m, 67.88H), 0.89 - 0.82 (m, 4.58 H).

¹³C NMR (100 MHz, CDCl₃, δ in ppm): 156.93, 156.36, 154.35, 130.50, 123.73, 112.79, 107.41, 99.53, 99.29, 95.94, 69.78, 69.32, 29.65, 29.00, 26.33, 0.18.

MS: [M+H]⁺ Calculated for C₁₅₀H₁₅₆F₂₄N₁₂O₁₂ 2774.16. Found 2774.10.

Elemental analysis (%): Calculated C 64.93 H 5.67 N 6.06. Found C 64.93 H 5.38 N 5.66.

Compound 2 (0.55 g, Yield: 57%)

UV-vis (nm): 281, 311, 450.

¹H NMR (400 MHz, CDCl₃, δ in ppm): 7.84 (s, 6H), 7.42 (d, 8.03H, J = 8 Hz), 7.20 (t, 6.02H, J = 8 Hz), 6.98 (s, 11.87H), 6.76 (d, 4.02H, J = 1.84 Hz), 4.23 (t, 11.99H, J = 8, 4 Hz), 3.97 (t, 8.88H, J = 8, 4 Hz), 3.88 (t, 3.17H, J = 8, 4 Hz), 2.00 - 1.88 (m, 12.39H), 1.81 - 1.7 (m, 12.28H), 1.39 (d, 68.31H, J = 24 Hz), 0.96 (d, 0.37H, J = 4 Hz), 0.90 - 0.83 (m, 2.36H).

¹³C NMR (100 MHz, CDCl₃, δ in ppm): 160.31, 159.85, 149.08, 140.42, 135.41, 130.23, 129.38, 127.03, 123.73, 116.00, 113.69, 69.79, 69.13, 29.66, 29.09, 26.34.

MS: [M]⁺ Calculated for C₁₅₀H₁₅₆Cl₂₄N₁₂O₁₂ 3169.43. Found 3169.48.

Elemental analysis (%): Calculated C 56.84 H 4.96 N 5.30. Found C 56.53 H 5.32 N 5.07.

Compound 3 (0.65 g, Yield: 72%)

UV-vis (nm): 281, 315, 435.

¹H NMR (400 MHz, CDCl₃, δ in ppm): 7.83 (s, 6H), 7.38 (d, 4.06H, J = 8 Hz), 7.32 (d, 2.09H, J = 8 Hz), 7.20 - 7.08 (m, 6.05H), 6.65 (d, 1.90H, J = 10.52 Hz), 6.59 - 6.55 (m, 6.02H), 6.52 - 6.47 (m, 6.03H), 6.40 - 6.31 (m, 4.09H), 4.34 - 4.21 (m, 12H), 3.98 (quint, 8.71H, J = 4, 8, 8, 4 Hz), 3.89 - 3.78 (m, 3.30H), 1.94 (d, 12.12H, J = 8 Hz), 1.81 - 1.70 (m, 12.10H), 1.56 (s, 10.68H), 1.43 - 1.31 (m, 58.93H), 0.96 (d, 0.19H, J = 8 Hz), 0.90 - 0.82 (m, 1.24H).

¹³C NMR (100 MHz, CDCl₃, δ in ppm): 162.89, 159.16, 156.61, 149.08, 129.18, 126.85, 123.71, 107.39, 101.67, 99.58, 99.78, 69.76, 69.37, 29.64, 28.96, 26.31.

MS: [M+H]⁺ Calculated for C₁₅₀H₁₅₆F₁₂Cl₁₂N₁₂O₁₂ 2973.80. Found 2973.82.

Elemental analysis (%): Calculated C 60.61 H 5.29 N 5.65. Found C 60.98 H 5.29 N 5.29.

2. NMR Spectra

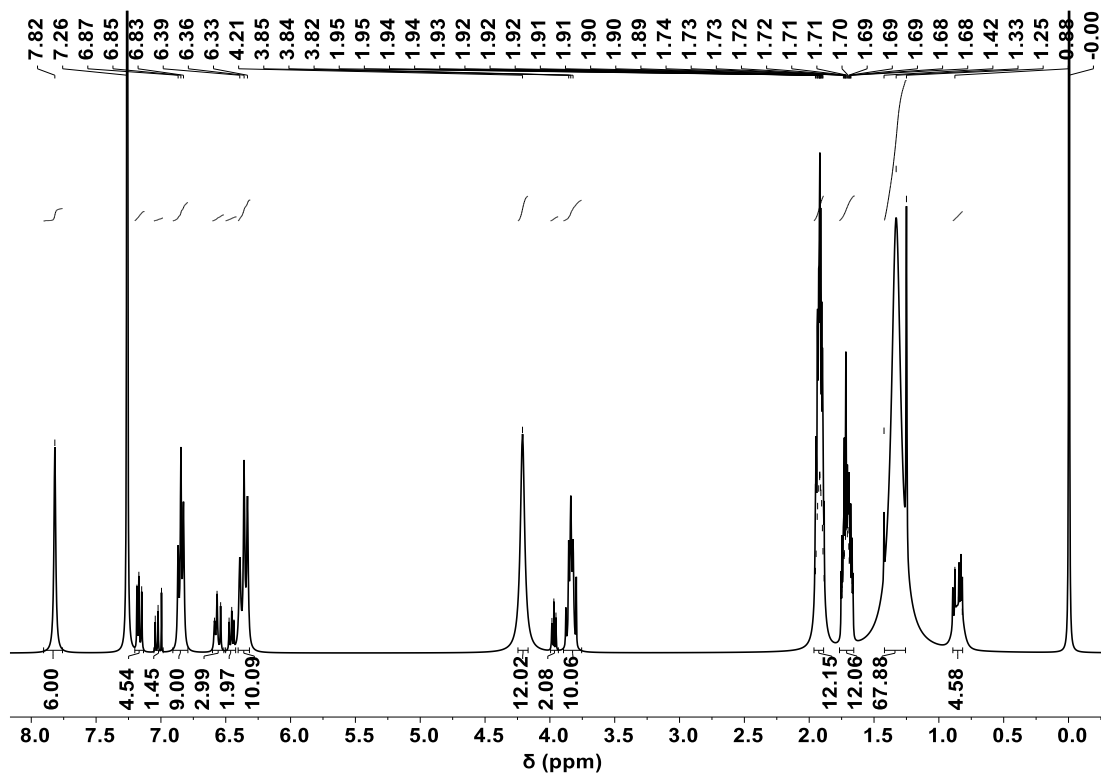


Figure S1. ¹H NMR spectrum of compound 1.

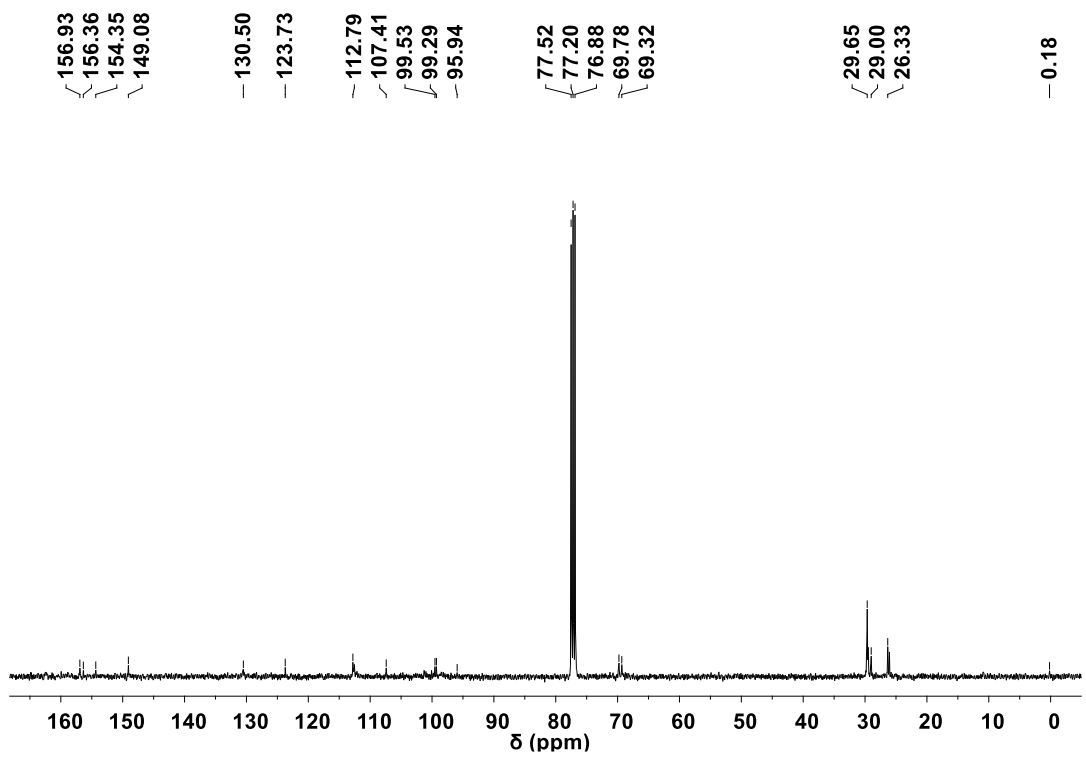


Figure S2. ^{13}C NMR spectrum of compound **1**.

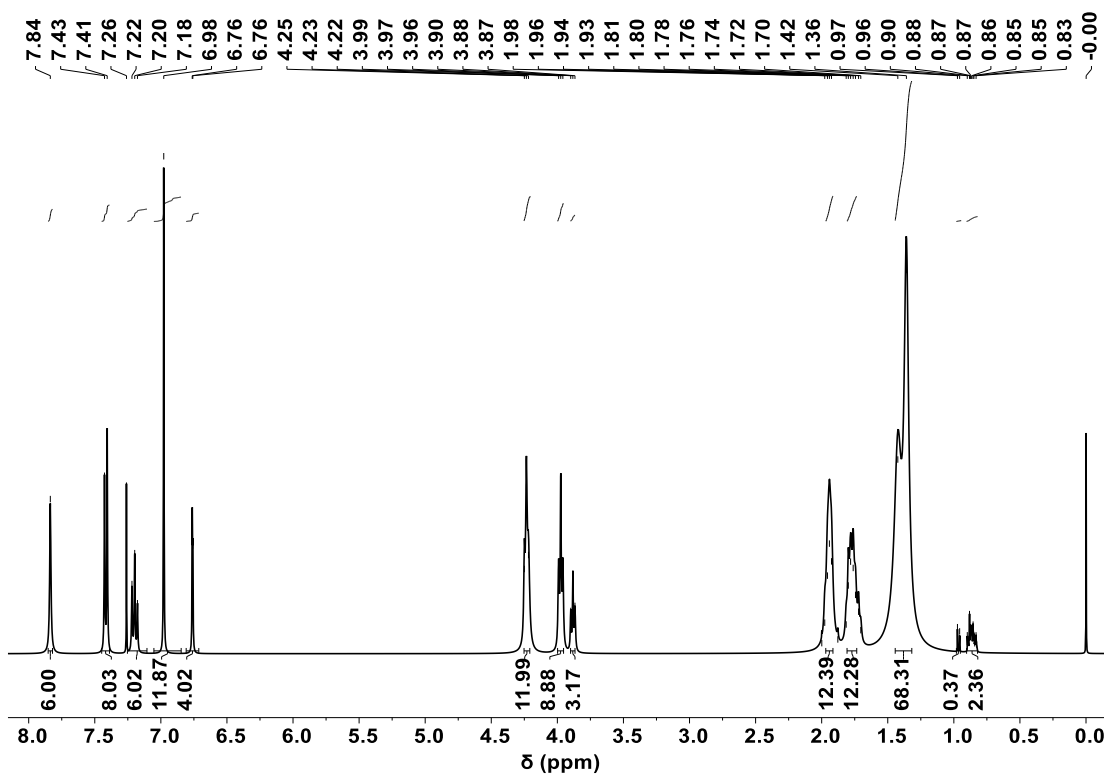


Figure S3. ^1H NMR spectrum of compound **2**.

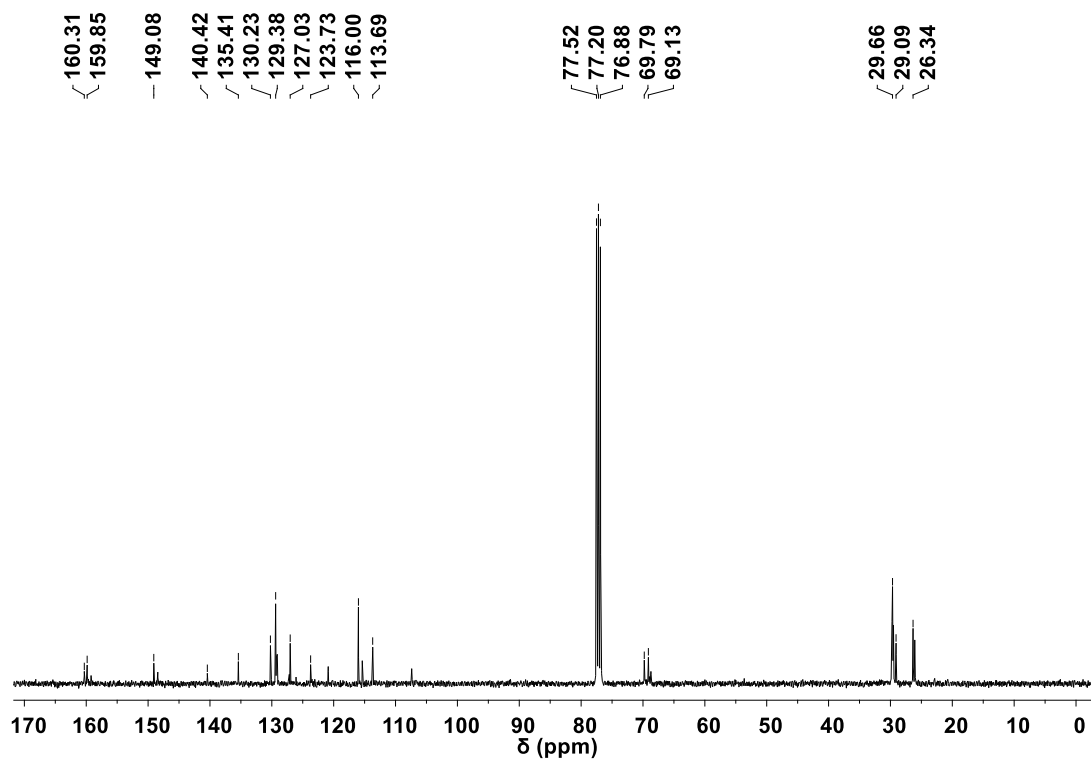


Figure S4. ^{13}C NMR spectrum of compound 2.

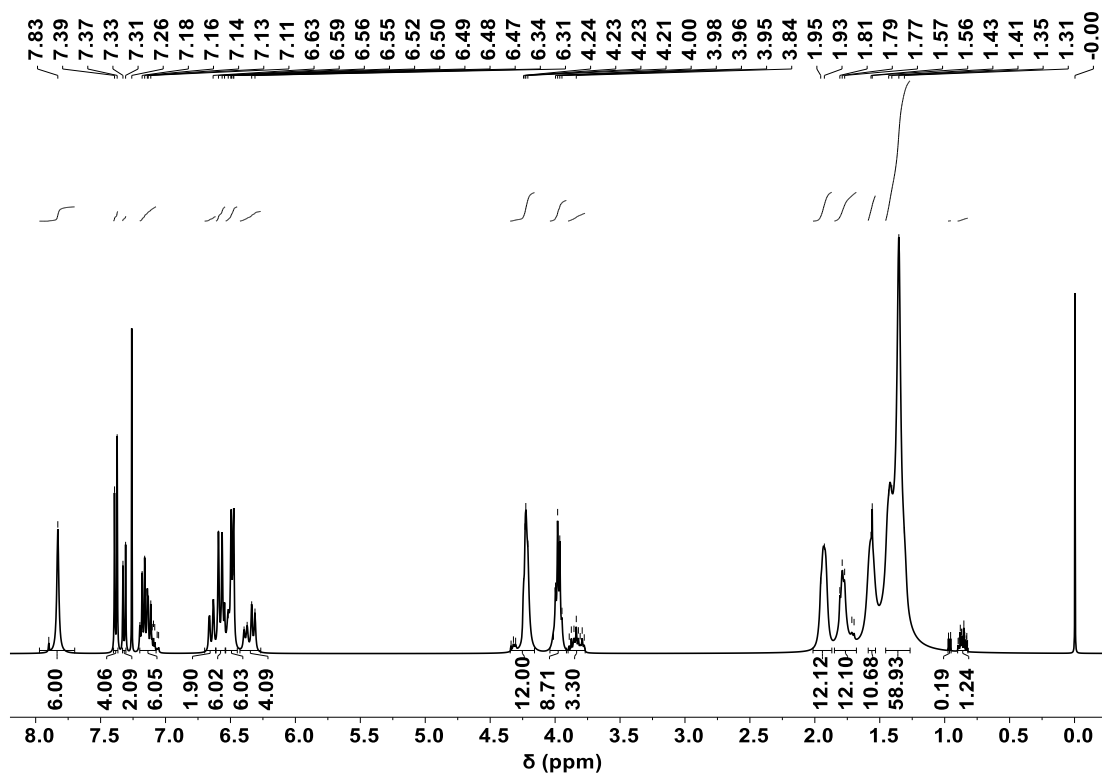


Figure S5. ^1H NMR spectrum of compound 3.

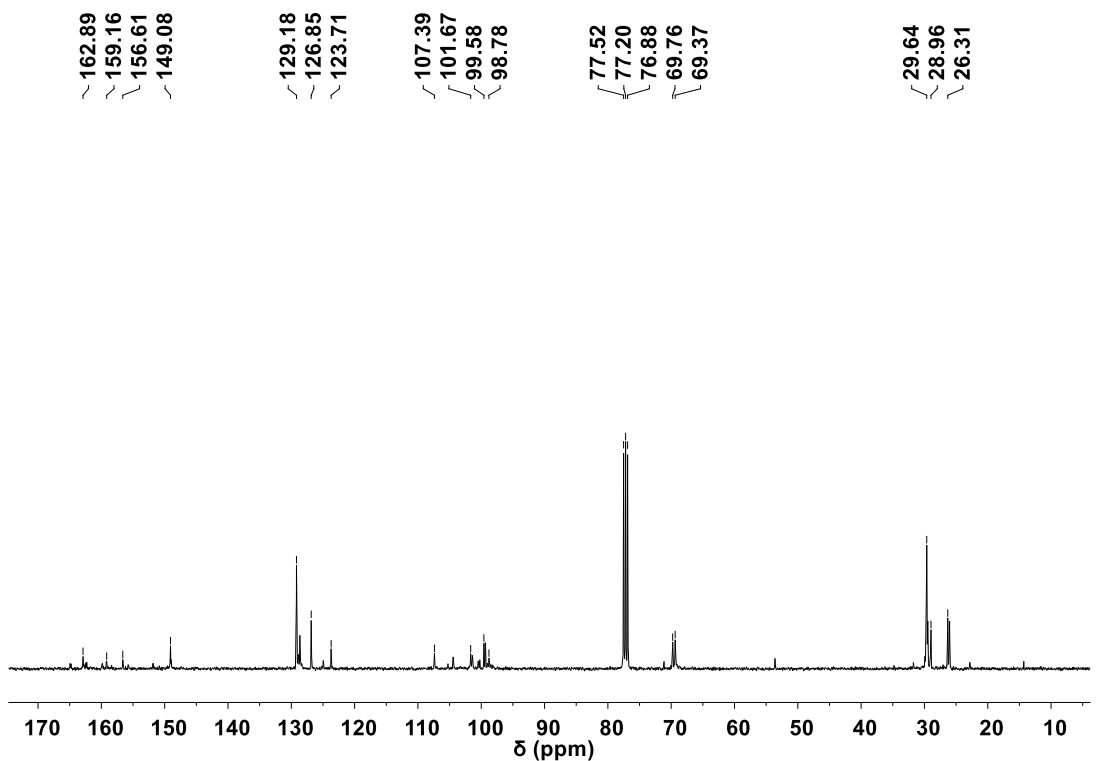


Figure S6. ^{13}C NMR spectrum of compound **3**.

3. TGA Curves

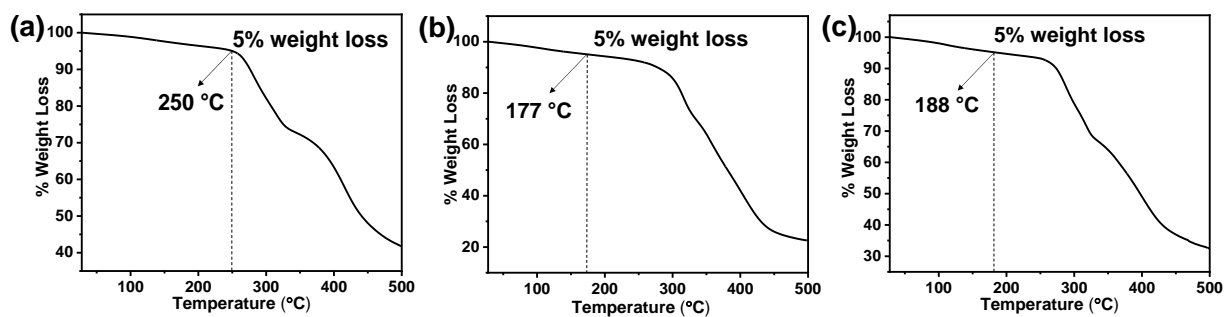


Figure S7. TGA curves of compounds (a) **1**, (b) **2** and (c) **3**. The measurements were performed under a nitrogen atmosphere, with a heating rate of 10 °C/min.

4. DSC Analysis

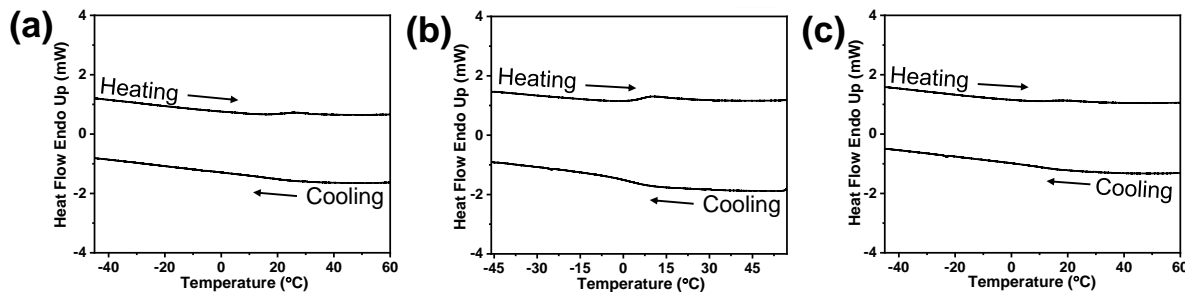


Figure S8. DSC thermograms of compound (a) **1**, (b) **2** and (c) **3** on heating and cooling cycles at the rate of 5 °C/min.

Table S1. Thermal behavior of the synthesized compounds **1-3**^{a, b, c}

| Compound | Heating Scan | Cooling Scan |
|----------|------------------------------------|-------------------------------------|
| 1 | Cr 25.9 (4.04) N _D 60 I | I 40 N _D (0.84) 23.2 Cr |
| 2 | Cr 9.9 (5.81) N _D 60 I | I 40 N _D (1.57) 7.35 Cr |
| 3 | Cr 18.2 (5.23) N _D 60 I | I 40 N _D (1.10) 17.45 Cr |

^a Phase transition temperature (peak) in °C and transition enthalpies in kJmol⁻¹ (in parentheses).

^b Phase assignments: Cr = Crystalline, N_D = discotic nematic, I = isotropic.

^c Mesophase to isotropic (on heating) and from isotropic to mesophase (on cooling) were observed from POM only.

5. POM & WAXS Studies

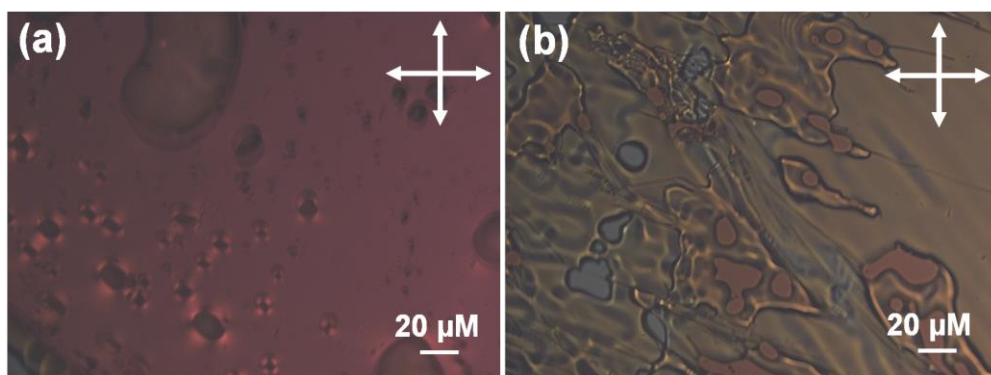


Figure S9. Cross-polarized optical microscopic images of compound (a) **2** and (b) **3** (scale bar = 20 μm); in the mesophase upon cooling to 25 °C from isotropic phase.

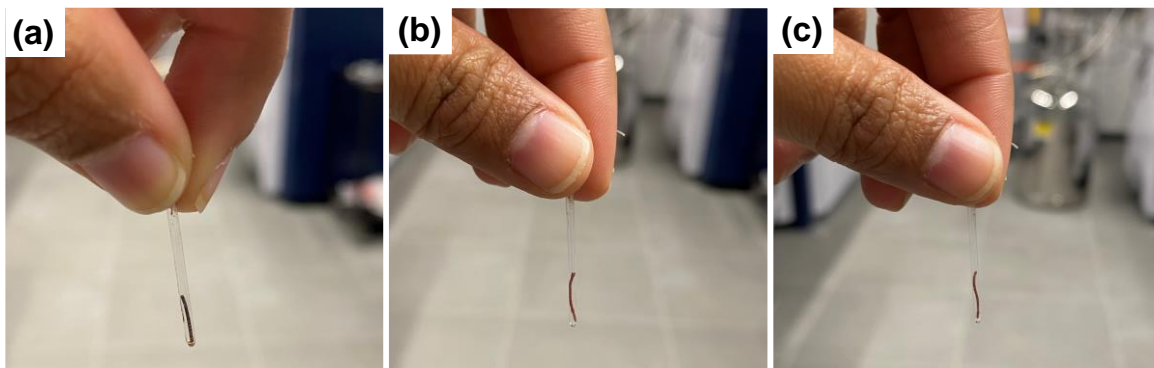


Figure S10. Images of aligned fibers of compound (a) **1**, (b) **2** and (c) **3** obtained through a customized extruder and taken in capillaries for WAXS measurements.

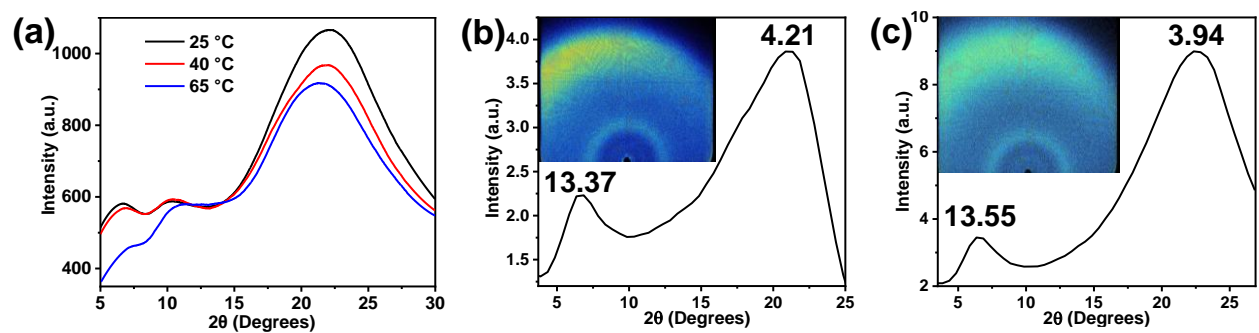


Figure S11. (a) Temperature dependent WAXS profile of compound **1** (unaligned). 1D profile of the WAXS pattern of aligned samples in the mesophase (2D profile in the inset) of compound (b) **2** and (c) **3** upon cooling to 25 °C from isotropic phase.

6. Photophysical Studies

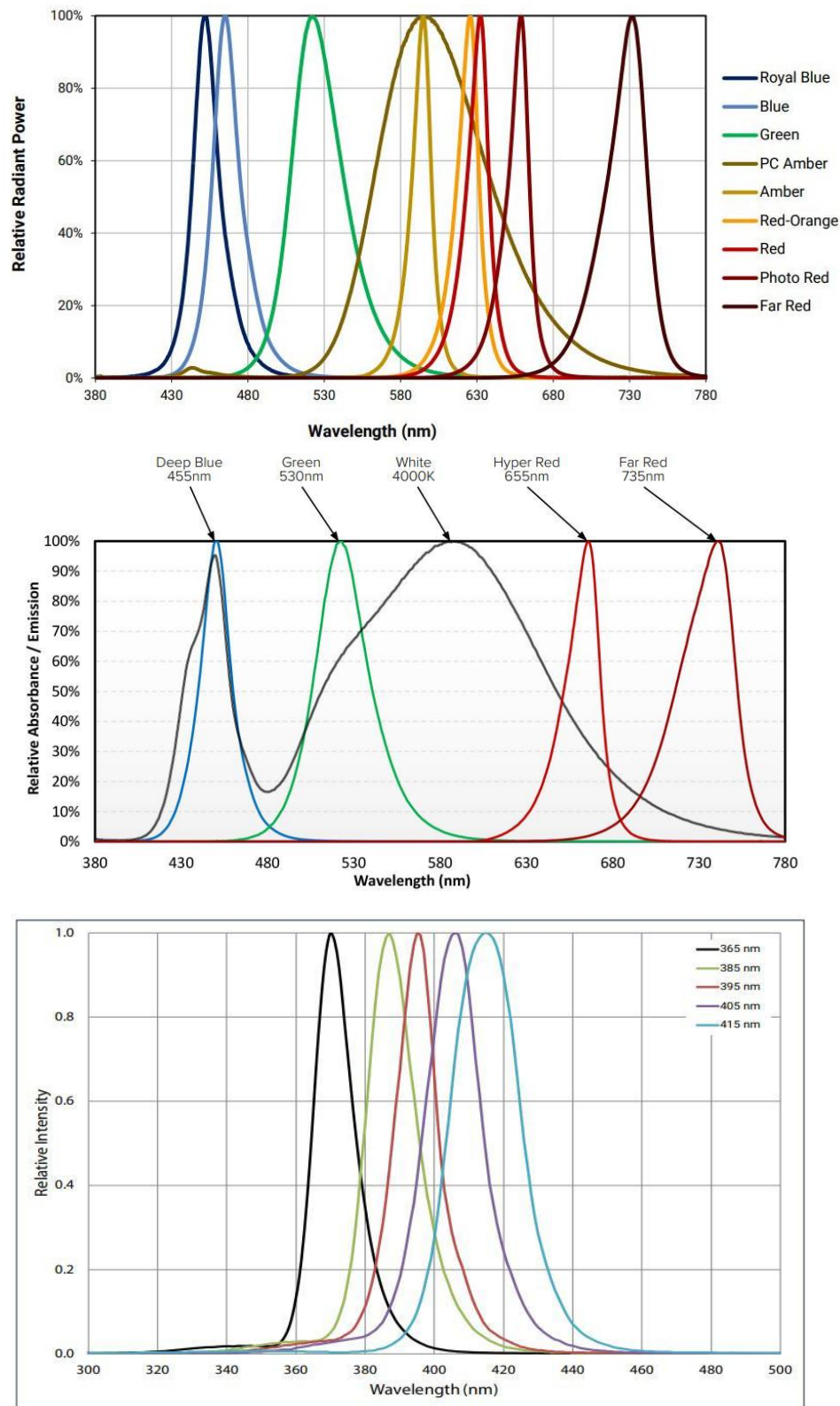


Figure S12. Emission Spectra of LEDs (as provided by Holmarc) used for the experiments.

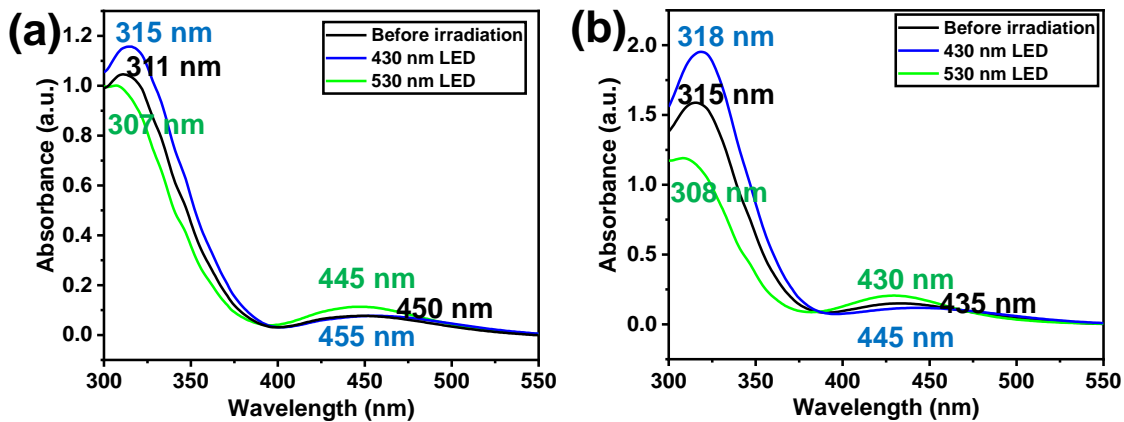


Figure S13. UV-vis absorption spectra of compounds (a) **2** and (b) **3** (10 μ M in Toluene), recorded without any irradiation and after irradiation with LEDs as mentioned in the inset.

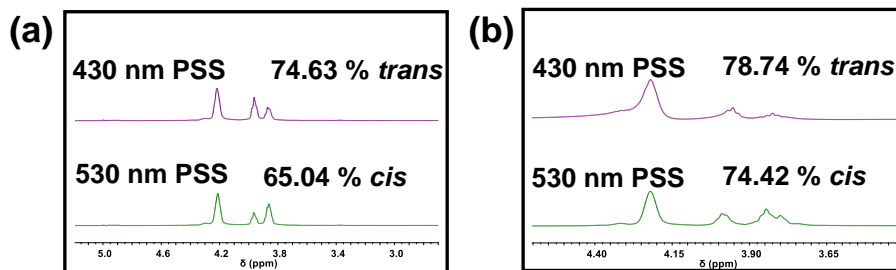


Figure S14. ^1H NMR spectra of (a) **2** and (b) **3** after irradiation with LEDs (as mentioned) to achieve the respective *E* and *Z* PSSs showing ratio of *E* and *Z* isomers.

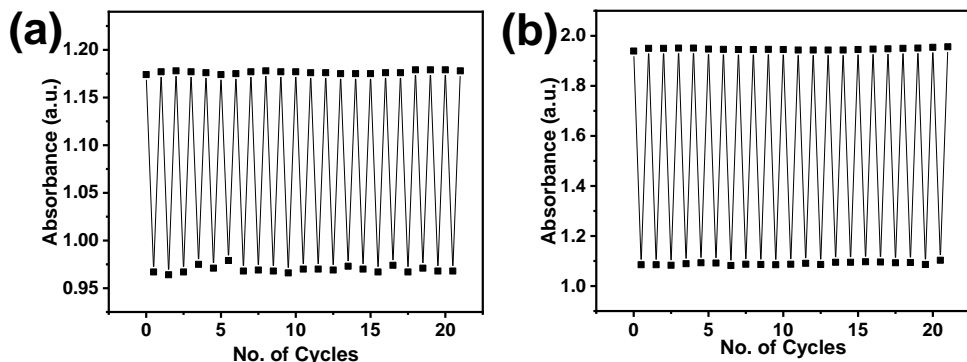


Figure S15. Cyclic photoisomerization of compounds (a) **2** and (b) **3** (10 μ M in Toluene) after alternating irradiation to obtain *Z* and *E* PSSs and recording absorbance at λ_{max} (315 and 318 nm, respectively) at 25 $^{\circ}\text{C}$.

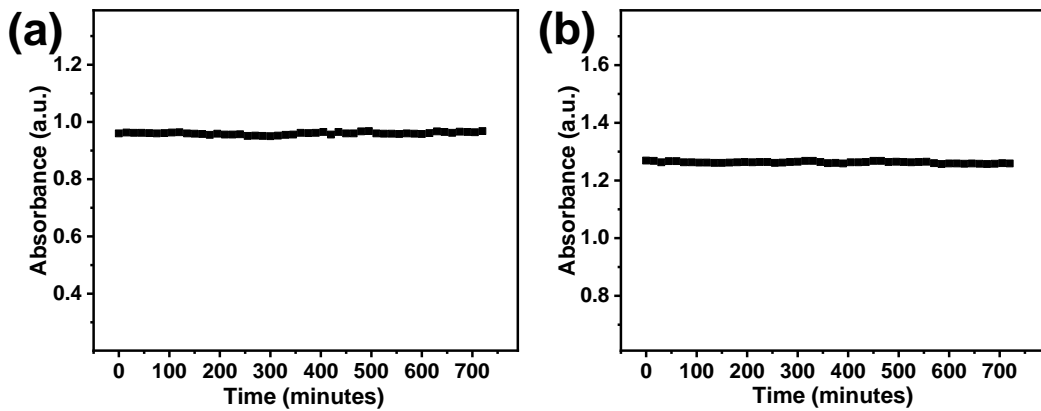


Figure S16. Photostability measurements of compounds (a) **2** and (b) **3** (10 μM in Toluene) carried out by 530 nm LED irradiation at 25 $^{\circ}\text{C}$ and recording absorbance at λ_{max} (315 and 318 nm, respectively) over 12 hours.

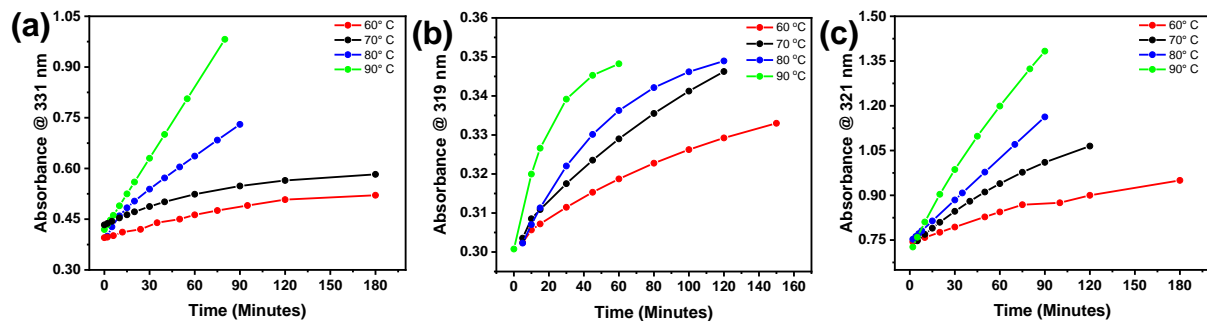


Figure S17. Absorbance at λ_{max} (as mentioned above) for thermal *Z* to *E* recovery of compounds (a) **1**, (b) **2** and (c) **3** (for 10 μM solutions) with time at different temperatures (as mentioned in the inset).

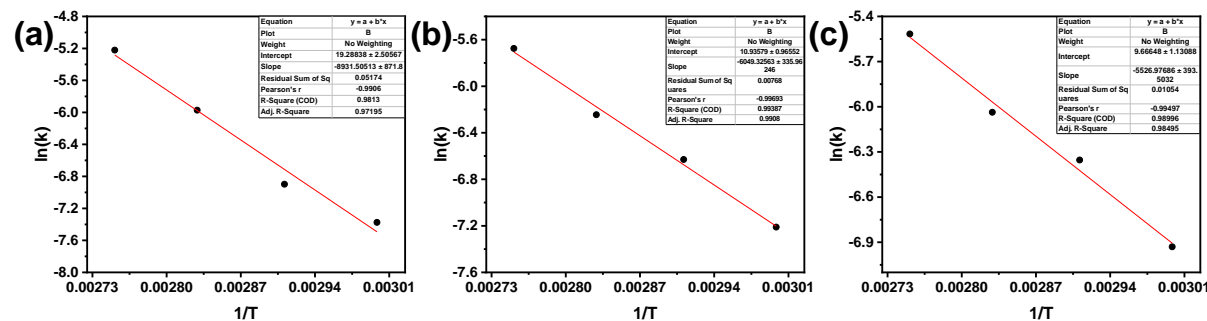


Figure S18. Arrhenius plots for thermal *Z* to *E* isomerization of compounds (a) **1**, (b) **2** and (c) **3** (for 10 μM solutions).

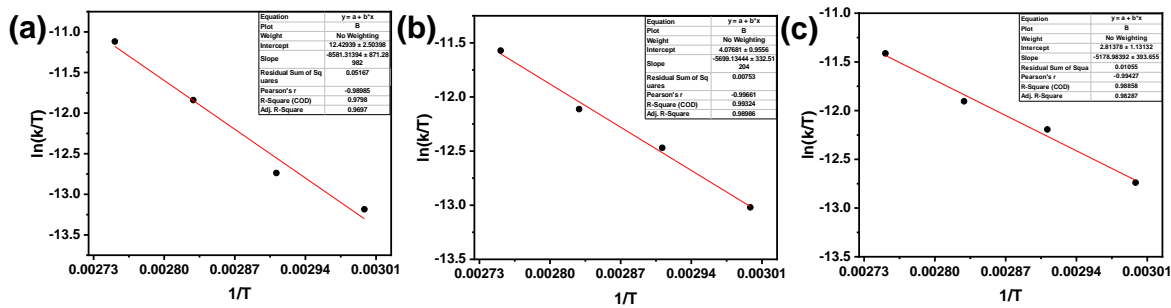


Figure S19. Eyring- Polanyi plots for thermal *Z* to *E* isomerization of compounds (a) **1**, (b) **2** and (c) **3** (for 10 μ M solutions).

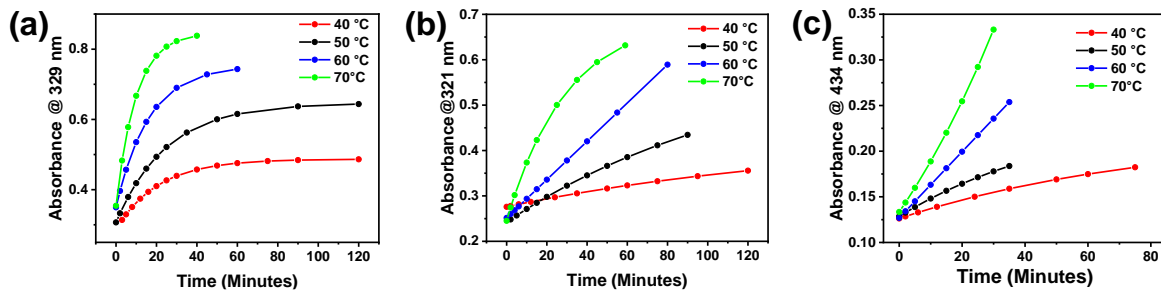


Figure S20. Absorbance at λ_{max} for thermal *Z* to *E* recovery of compounds (a) **1**, (b) **2** and (c) **3** in solid-state with time at different temperatures (as mentioned in the inset).

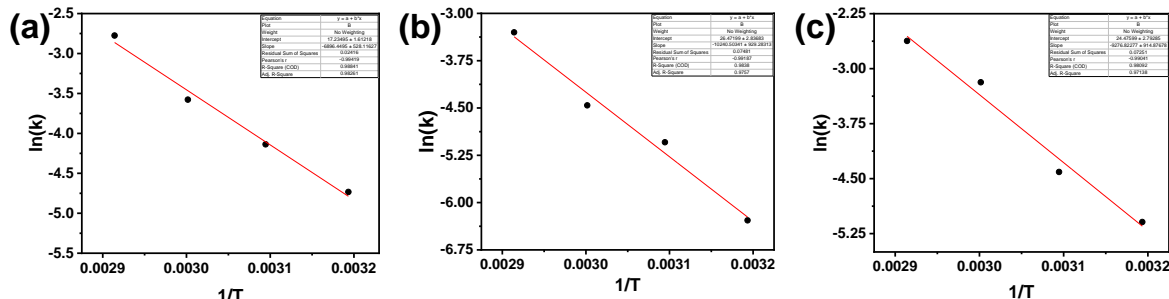


Figure S21. Arrhenius plots for thermal *Z* to *E* isomerization of compounds (a) **1**, (b) **2** and (c) **3** in solid-state.

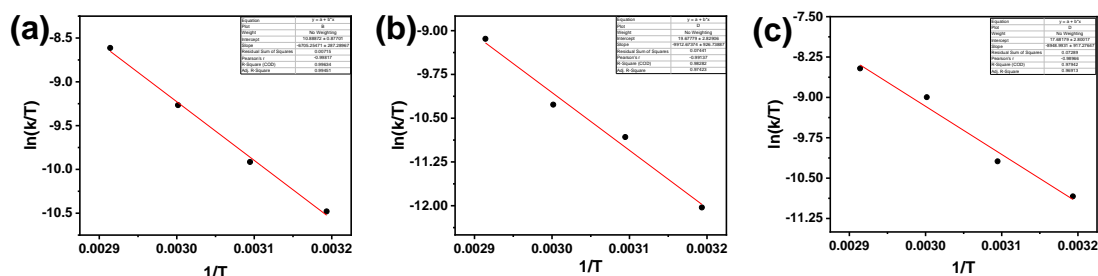


Figure S22. Eyring- Polanyi plots for thermal *Z* to *E* isomerization of compounds (a) **1**, (b) **2** and (c) **3** in solid-state.

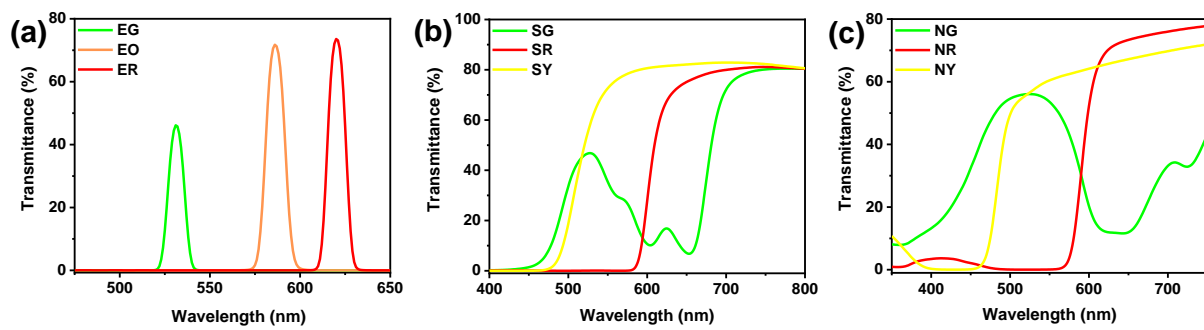


Figure S23. Transmittance spectra of band pass filters from (a) Edmund optics, (b) Shopee and (c) Neewer, used for solar irradiation experiments.

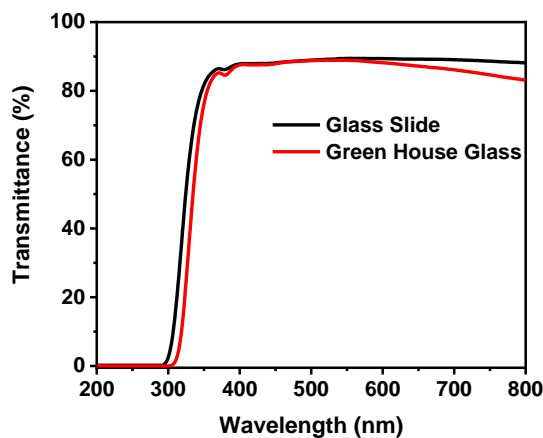


Figure S24. Transmittance spectra of glass slide used for thin film preparation and green house glass.

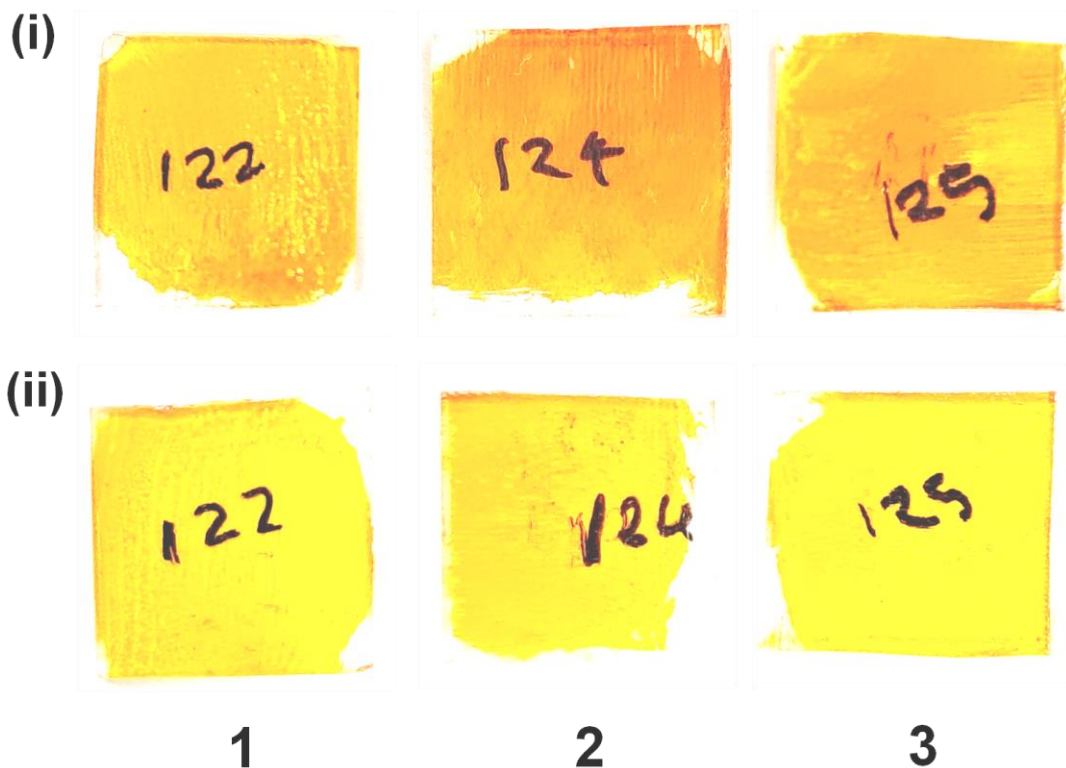


Figure S25. Thin films of compounds **1**, **2** and **3** where (i) indicates the films in their *E* isomer PSSs whereas (ii) indicates the film in their *Z* isomer PSSs.

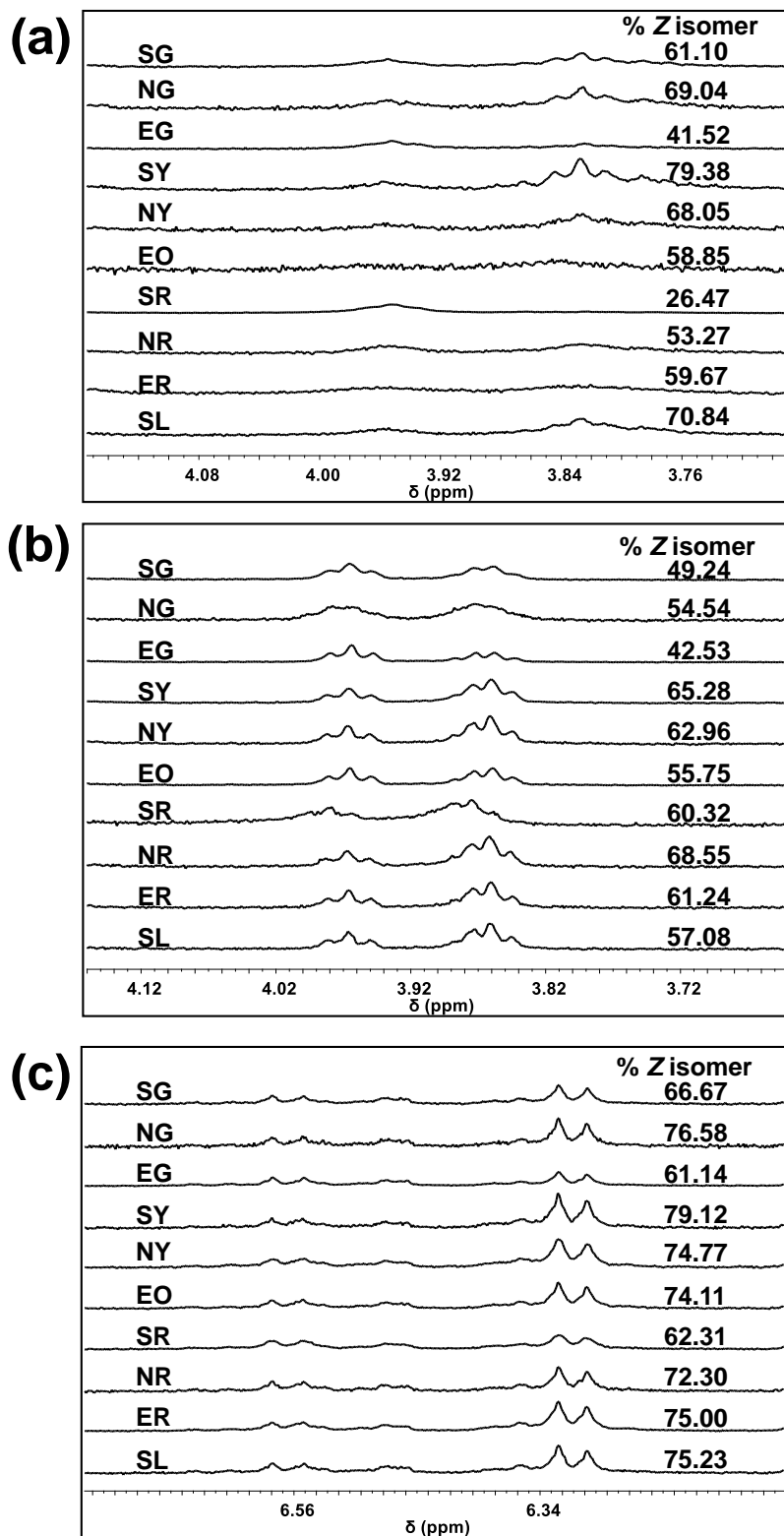


Figure S26. Percentage of Z isomer (as measured by ^1H NMR in CDCl_3) obtained for compound (a) **1**, (b) **2** and (c) **3** upon exposure to sunlight using various band pass filters for 5 hours. (Where E = Edmund, S = Shopee, N = Neewer, R = Red, O = Orange, Y = Yellow, G = Green, SL = Direct Sunlight). Average temperature inside the green house was found to be 50.2 °C and the average intensity of sunlight observed was 635 W/m².

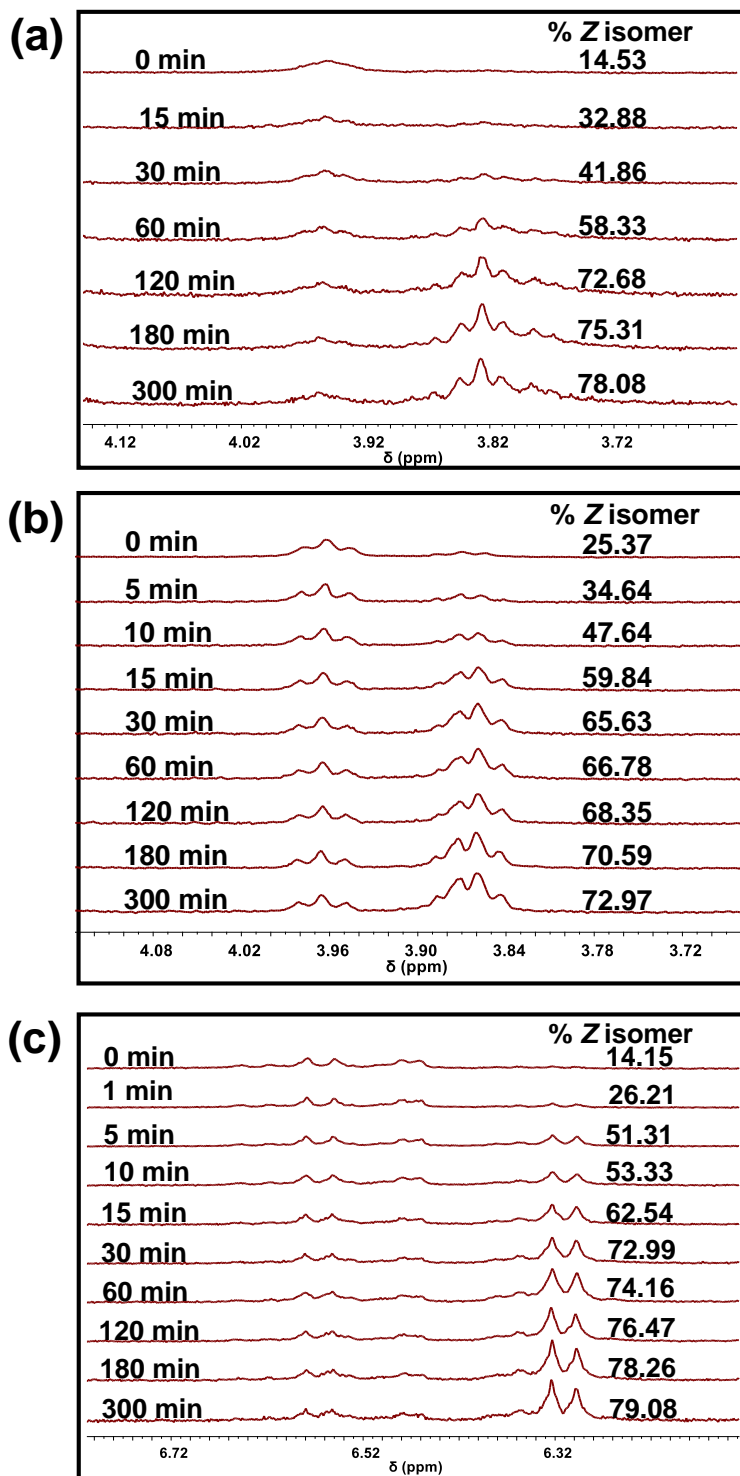


Figure S27. Percentage of Z isomer (as measured by ^1H NMR in CDCl_3) obtained in thin films of compound (a) **1**, (b) **2** and (c) **3** upon sunlight irradiation through SY filter over 5 hours. Average temperature inside the green house was found to be 51 °C and the average intensity of sunlight observed was 598 W/m 2 .

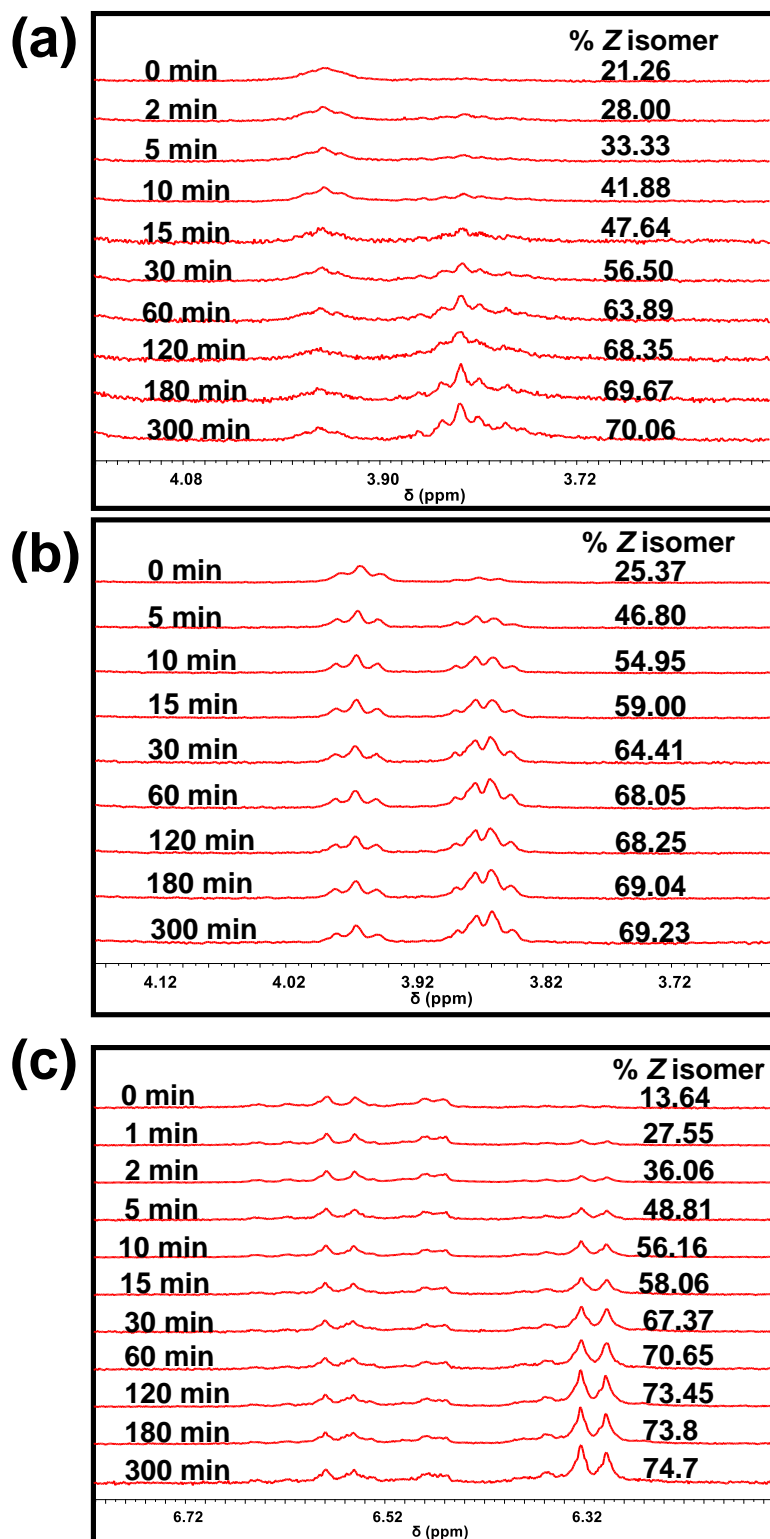


Figure S28. Percentage of Z isomer (as measured by ^1H NMR in CDCl_3) obtained in thin films of compound (a) **1**, (b) **2** and (c) **3** upon direct sunlight irradiation over 5 hours. Average temperature inside the green house was found to be 52 $^{\circ}\text{C}$ and the average intensity of sunlight observed was 560 W/m^2 .

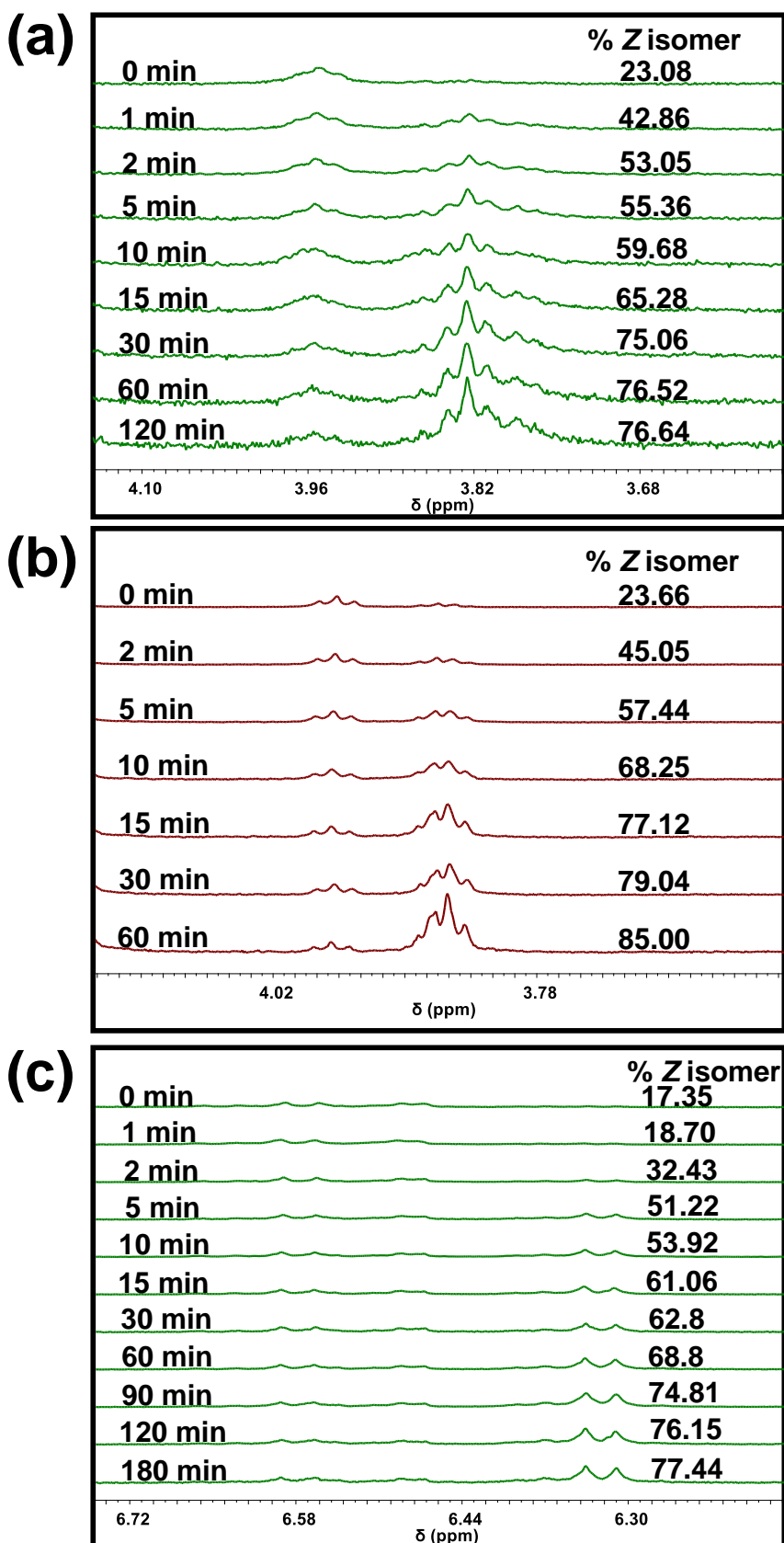


Figure S29. Percentage of Z isomer (as measured by ^1H NMR in CDCl_3) in thin films of compound (a) **1**, (b) **2** and (c) **3** upon LED irradiation (530 nm for **1** & **3**, 625 nm for **2**).

Calculation of solar energy conversion efficiency

The solar energy conversion efficiency (η) is estimated under AM 1.5 solar irradiation spectrum as per previously reported method.^{3,4}

$$\eta = \frac{\frac{\Phi_{E-z} \cdot \Delta H_{iso}}{hcN_A} \int_{\lambda_1}^{\lambda_2} E_{AM} \text{1.5}(\lambda) \lambda \cdot d\lambda}{\int_{280}^{4000} E_{AM} \text{1.5}(\lambda) \lambda \cdot d\lambda}$$

Where, Φ_{E-z} = quantum yield; ΔH_{iso} = enthalpy of isomerization, λ_1 and λ_2 are the bandwidth of the filter used for solar experiments, h = Planck's constant; c = speed of light; and N_A = Avogadro's number.

Quantum yield (ϕ) of photoisomerization was calculated by using previously established methods from literature.⁵⁻⁷ To determine quantum yield, we prepared 10 μM solution of compound **1-3** in either toluene or DMSO and irradiated with 530 nm LED. Absorption spectra is recorded thereafter at different time intervals.

Quantum yield is calculated from the following equation,

$$\Phi = \frac{V y_\infty R_0}{I \cdot l \cdot \epsilon_E}$$

Where, Φ = quantum yield; V = sample volume; ϵ_E = molar extinction coefficient; l = path length; and I = molar photon flux, R_0 and y_∞ obtained from plotting the fraction of cis-isomers as a function of time from UV absorption spectra.

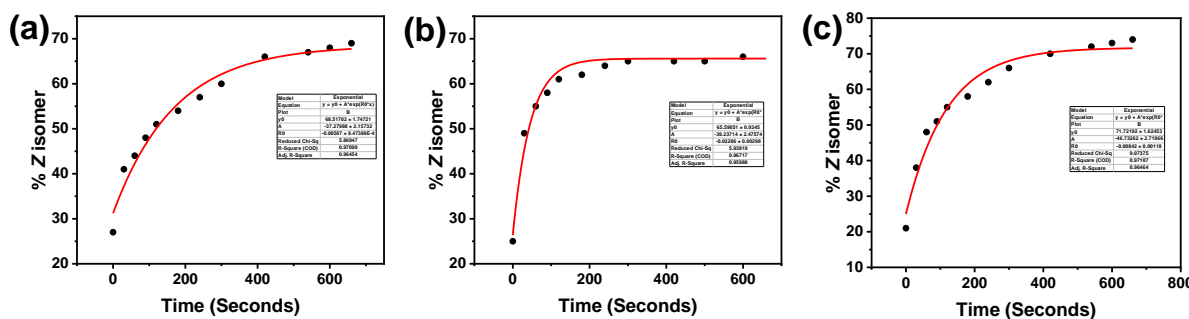


Figure S30. The fitting result of Z-isomer fraction of compound (a) **1**, (b) **2** and (c) **3** after green light irradiation.

Calculation of Molar Photon Flux

Molar photon flux of 530 nm light was calculated using equation

$$I = \frac{P\lambda}{hcN_A}$$

where P = power (of the light used); λ = incident light wavelength; h = Planck's constant; c = speed of light; and N_A = Avogadro's number.

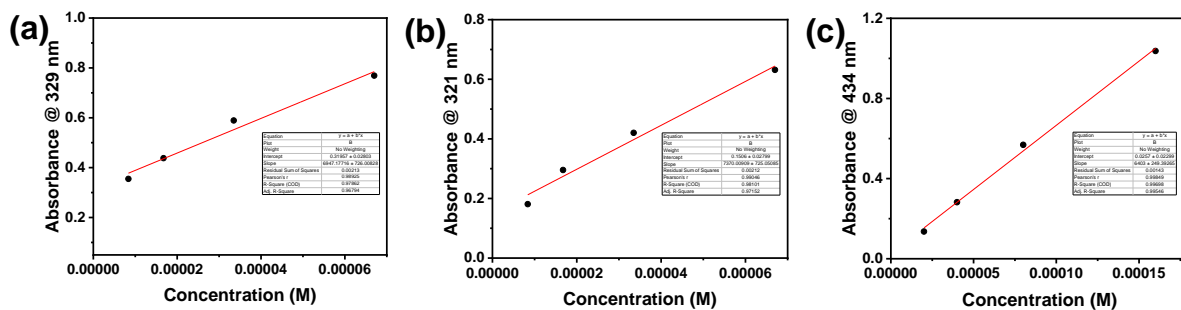


Figure S31. Absorption at λ_{max} for compounds (a) **1**, (b) **2** and (c) **3** at different concentrations.

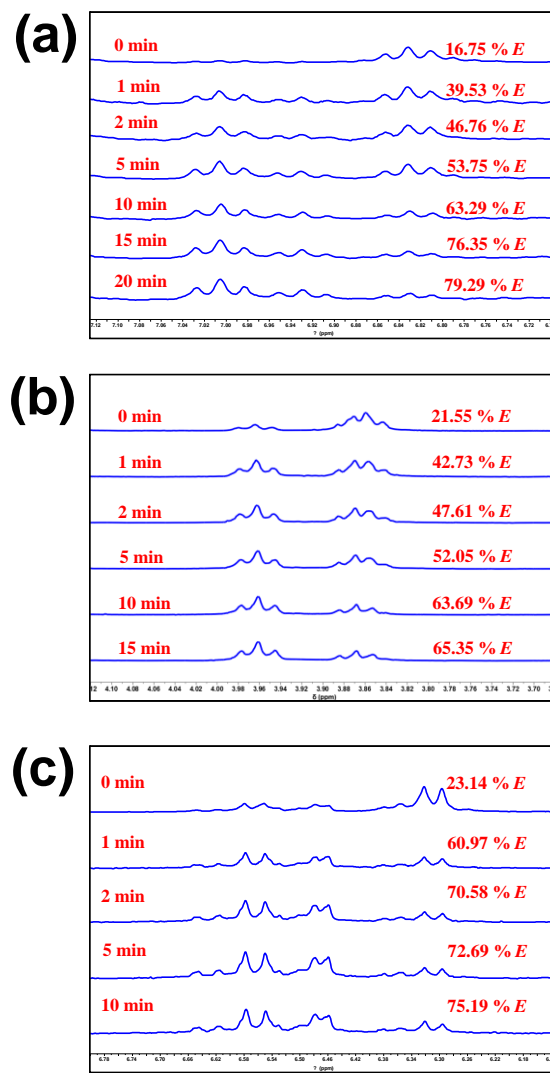


Figure S32. Percentage of *E* isomer (as measured by ^1H NMR in CDCl_3) in thin film of compounds (a) **1**, (b) **2** and (c) **3** upon irradiation with LEDs (430 nm for **1** & **3**, 395 nm for **2**).

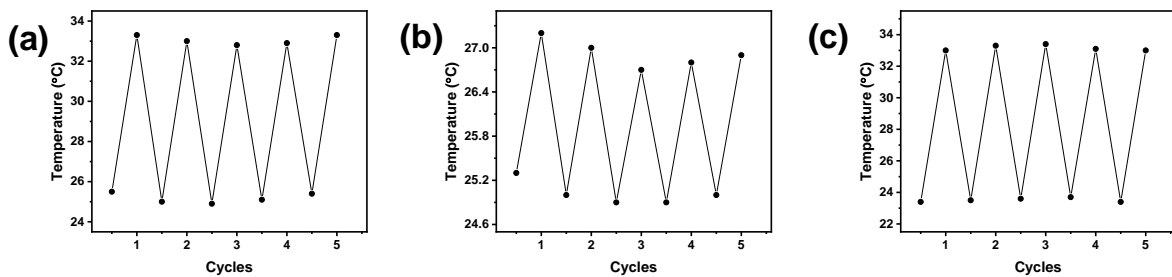


Figure S33. Maximum temperature observed on the surface of the films (a) **1**, (b) **2** and (c) **3**, during the five consecutive charging and discharging cycles.

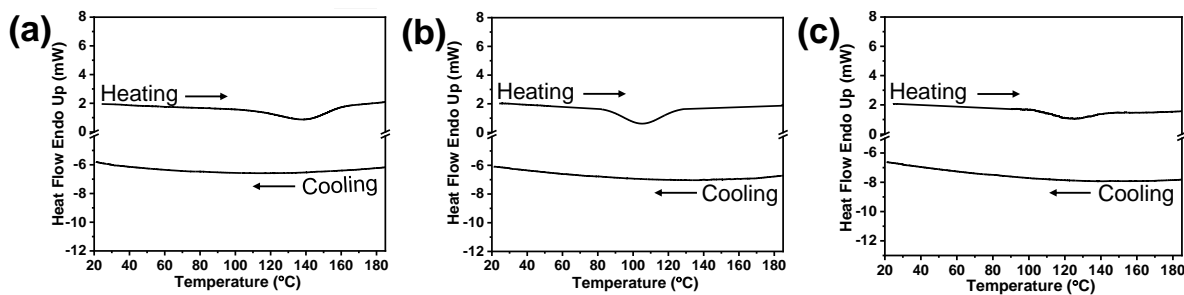


Figure S34. DSC thermogram obtained on heating and subsequent cooling compound (a) **1**, (b) **2** and (c) **3** in its Z PSS at the rate of 5 °C/min.



Figure S35. IR thermal camera images of heat release from (a) *E*-rich film and (b) *Z*-rich film (prepared by 3mg sample) of compound **3** on irradiation with 430 nm LED.

References:

1. A. K. KM, S. Sony, S. Dhingra, M. Gupta, *ACS Mater. Lett.* **2023**, *5*, 3248–3254.
2. G. Yeap, M. A. Rahim, C. M. Lin, H. Lin, N. Maeta, M. Ito, *J. Mol. Liq.* **2016**, *223*, 734–740.

3. W. Sun, Z. Shangguan, X. Zhang, T. Dang, Z.-Y. Zhang, T. Li, *ChemSusChem* **2023**, *16*, e202300582.
4. Y. Shi, M. A. Gerkman, Q. Qiu, S. Zhang, G. G. D. Han, *J. Mater. Chem. A* **2021**, *9*, 9798–9808.
5. X. Xu, B. Wu, P. Zhang, Y. Xing, K. Shi, W. Fang, H. Yu, G. Wang, *ACS Appl. Mater. Interfaces* **2021**, *13*, 22655–22663.
6. Y. He, Z. Shangguan, Z. Zhang, M. Xie, C. Yu, T. Li, *Angew. Chem. Int. Ed.* **2021**, *60*, 16539–16546.
7. A. Dolai, S. Bhunia, K. Manna, S. Bera, S. M. Box, K. Bhattacharya, R. Saha, S. Sarkar, S. Samanta, *ChemSusChem* **2024**, e202301700.